Heliyon 10 (2024) e23705

Contents lists available at ScienceDirect

Heliyon

journal homepage: www.cell.com/heliyon

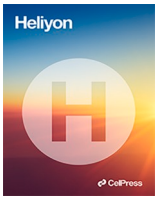

Impact of CT-guided hookwire localization on tumor spread through air spaces in stage IA lung adenocarcinoma

Xiaofan Wang [a,2], Xiaoxiao Dai [b,2], Qifeng Ding [a,2], Yi Xu [a], Lei Chen [a], Shanzhou Duan [a], Yongsheng Zhang [b], Yongbing Chen [a,1,**], Donglai Chen [c,*,1]

[a] Department of Thoracic Surgery, The Second Affiliated Hospital of Soochow University, Suzhou, 215004, China
[b] Department of Pathology, The Second Affiliated Hospital of Soochow University, Suzhou, 215004, China
[c] Department of Thoracic Surgery, Zhongshan Hospital, Fudan University, Shanghai, 200032, China

ARTICLE INFO

Keywords:
CT-Guided hookwire localization
Lung adenocarcinoma
Spread through air spaces

ABSTRACT

Background: It remains undetermined whether preoperative computed tomography (CT)-guided hookwire localization would result in elevated risk of tumor spread through air spaces (STAS) in stage IA lung adenocarcinoma.

Methods: A total of 1836 patients who underwent lobectomy were included. To eliminate the potential impact of confounding factors on producing STAS, propensity score–matching (PSM) was used to create two balanced subgroups stratified by implementation of hookwire localization. We also introduced an external cohort including 1486 patients to explore the effect of hookwire localization on the incidence of STAS and patient survival after sublobar resection (SR). For proactive simulation of hookwire localization, 20 consecutive lobectomy specimens of p-stage IA lung adenocarcinoma were selected.

Results: Ex vivo tests revealed that mechanical artifacts presenting as spreading through a localizer surface (STALS) could be induced by hookwire localization but be distinguished by CD68 and AE1/3 antibody-based immunohistochemistry. The distance of STALS dissemination tended to be shorter compared with real STAS ($P = 0.000$). After PSM, implementation of hookwire localization was not associated with elevated STAS incidence, nor worse survival in p-stage IA patients undergoing lobectomy irrespective of STAS.

Conclusions: CT-guided hookwire localization might induce mechanical artifacts presenting as STALS which could be distinguished by immunohistochemistry, but would not affect survival in p-stage IA disease. Surgeons can be less apprehensive about performing hookwire localization in relation to STAS on stage IA disease suitable for SR.

1. Introduction

Tumor spread through air spaces (STAS), first described in lung tumors by Kadota and his colleagues in 2015 [1], is defined as the

* Corresponding author.
** Corresponding author.
E-mail addresses: chentongt@sina.com (Y. Chen), allen_stcdl2006@163.com (D. Chen).
[1] Drs. Donglai Chen and Yongbing Chen are listed as co-senior authors.
[2] Drs. Wang X., Dai X. and Ding Q. equally contributed to the work.

https://doi.org/10.1016/j.heliyon.2023.e23705
Received 25 August 2023; Received in revised form 11 December 2023; Accepted 11 December 2023
Available online 17 December 2023

spread of tumor cells as micropapillary clusters, solid nests, or single cells into air spaces in the lung parenchyma adjacent to and beyond the edge of the main tumor. Despite the controversies regarding STAS as a possible ex vivo artifact during specimen processing [2], STAS is predominantly identified as an important prognostic factor associated with decreased recurrence-free survival (RFS) and overall survival (OS) [3,4] in various types and stages of non-small cell lung cancer (NSCLC) [4–6].

Recently, not only JCOG0802 [7] but also CALGB140503 [8] suggested similar oncologic outcomes of sublobar resection (SR) as an alternative to lobectomy in small-sized NSCLCs. However, the information on the positive rate of STAS was unavailable in both JCOG0802 and CALGB140503. To be noted, previous studies have suggested that lobectomy might offer better outcomes than SR in STAS-positive T1 disease [9,10]. Given that preoperative localization of the target lesions plays a key role in performing SR, in the context of possible tumor dissemination by mechanical forces, it remains undetermined regarding the potential association between preoperative hookwire localization and presence of STAS in stage IA lung adenocarcinoma.

In this study, we aimed to investigate whether preoperative CT-guided hookwire localization affected the incidence of STAS in stage IA lung adenocarcinoma, and to determine the impact of CT-guided hookwire localization on patient survival.

2. Materials and methods

2.1. Prospective simulated localized lesions and STAS

To assess whether the mechanical force by hookwire localizer possibly resulted in tumor cells spreading through a localizer surface (STALS), we prospectively selected 20 gross specimens before dipping them into formalin. These specimens were diagnosed as STAS-negative lesions by intraoperative frozen sections and further confirmed by paraffin-embedded ones. After penetrating the lesion ex vivo using a hookwire localizer, we observed whether presence of STALS could be produced in the precancerous tissues in hematoxylin and eosin (HE)-stained sections under microscope (Supplemental Figs. 1A–B).

2.2. Patient selection

The ethics committee of the Second Affiliated Hospital of Soochow University approved this study (IRB: JD-HG-2022-25). All the included patients obtained informed consent and signed a consent form for preoperative CT-guided hookwire localization.

A primary cohort was included which consisted of 2317 patients with stage IA invasive adenocarcinoma (IAC) presenting as pulmonary nodules who underwent R0 pulmonary resection at the Second Affiliated Hospital of Soochow University in China from March 2017 to December 2021. To minimize data bias by confounding factors, propensity-score matching (PSM) was applied to create balanced groups with respect to patient-, operative-, and histology-level confounders and resulted in two groups stratified by implementation of preoperative CT-guided hookwire localization. The hookwire localization (HL) group was also categorized into three subgroups according to the relative spatial position relations between localization site and main tumor. We also introduced an external cohort from our previous study [11] to explore the effect of hookwire localization on the incidence of STAS and patient survival after SR. The pathological stage was based on the eighth edition of the American Joint Committee on Cancer TNM Staging Manual [12]. The exclusion criteria included: (1) patients who underwent neoadjuvant therapy; (2) patients with synchronous multiple NSCLCs or other primary malignancies.

2.3. Preoperative CT-guided hookwire localization

All imaging was performed by volume scanning with the same multidetector (16 slices) CT scanner (Siemens, Erlangen, Germany). Optimal puncture site, angle and route were determined from previous CT scans, avoiding the ribs, scapula, large blood vessels, fissure of the lung and lung bullae. Laser cross-positioning was used to pinpoint the location of the hookwire insertion site on the body surface. The insertion length and angle were estimated on the initial CT images, and the localizer was then inserted without penetrating the pleura. Afterwards, repeated CT scans were obtained to confirm or redirect the localizer to obtain adequate accuracy of nodule localization. Deviations of 2 cm or less between the localizer and the center of the target nodule were considered sufficiently accurate to allow for safe nodule localization [13]. Once the relative position of the hookwire and target nodule was acceptable, the hookwire was deployed into the lung parenchyma with its sheath retrieved [14,15], followed by a final control CT-scan.

2.4. Surgical procedures

All patients underwent video-assisted surgery (VATS) within 30 min after localization. The patient was placed in a lateral position for single-port VATS under general anesthesia. Wedge resection or segmentectomy of the localized area was performed, and the resected specimen with hookwire was retrieved with an endo bag via port incisions. The specimen was then delivered to the department of pathology for intraoperative frozen pathology which further guided subsequent resection strategy.

2.5. Histopathologic evaluation of STAS

Paraffin sections of resected tumor specimens were stained with hematoxylin and eosin and evaluated microscopically by pathologists independently. The pathologists were blinded to the patient information. The presence of STAS was reported as described in our previous studies [16,17], and its morphological subtypes were categorized into micropapillary clusters, solid nests and single cells

Table 1
Clinicopathological characteristics of the included patients with stage IA lung IAC before PSM and after PSM.

Variables	Before PSM (n = 3061)								After PSM (n = 1836)							
	STAS				CT-guided Hookwire Localization				STAS				CT-guided Hookwire Localization			
	No. of patients	Present (%)	Absent (%)	*P* value	No. of patients	With (%)	Without (%)	*P* value	No. of patients	Present (%)	Absent (%)	*P* value	No. of patients	With (%)	Without (%)	*P* value
Overall	2317	500 (21.6)	1817 (78.4)		2317	918 (39.6)	1399 (60.4)		1836	372 (20.3)	1464 (79.7)		1836	918 (50.0)	918 (50.0)	
Sex				0.183				0.081				0.958				1.000
Male	1238	254 (11.0)	984 (42.5)		1238	470 (20.3)	768 (33.1)		940	190 (10.3)	750 (40.8)		940	470 (25.6)	470 (25.6)	
Female	1079	246 (10.6)	833 (36.0)		1079	448 (19.3)	631 (27.2)		896	182 (9.9)	714 (38.9)		896	448 (24.4)	448 (24.4)	
Age (y)				0.550				0.012				0.415				1.000
≤52	1326	292 (12.6)	1034 (44.6)		1326	496 (21.4)	830 (35.8)		992	194 (10.6)	798 (43.5)		992	496 (27.0)	496 (27.0)	
>52	991	208 (9.0)	783 (33.8)		991	422 (18.2)	569 (24.6)		844	178 (9.7)	666 (36.3)		844	422 (23.0)	422 (23.0)	
Smoking				0.005				0.002				0.000				0.751
Non-smoker	1625	325 (14.0)	1300 (56.1)		1625	678 (29.3)	947 (40.9)		1350	243 (13.2)	1107 (60.3)		1350	678 (36.9)	672 (36.6)	
Current or former smoker	692	175 (7.6)	517 (22.3)		692	240 (10.4)	452 (19.5)		486	129 (7.0)	357 (19.4)		486	240 (13.1)	246 (13.4)	
Radiological feature				0.000				0.000				0.000				1.000
Subsolid	1607	292 (12.6)	1315 (56.8)		1607	678 (29.3)	929 (40.1)		1356	225 (12.3)	1131 (61.6)		1356	678 (36.9)	678 (36.9)	
Solid	710	208 (9.0)	502 (21.7)		710	240 (10.4)	470 (20.3)		480	147 (8.0)	333 (18.1)		480	240 (13.1)	240 (13.1)	
Primary site				0.000				0.000				0.000				0.000
RU	642	139 (6.0)	503 (21.7)		642	276 (11.9)	366 (15.8)		504	111 (6.0)	393 (21.4)		504	276 (15.0)	228 (12.4)	
RM	233	78 (3.4)	155 (6.7)		233	54 (2.3)	179 (7.7)		187	66 (3.6)	121 (6.6)		187	54 (2.9)	133 (7.2)	
RL	468	97 (4.2)	371 (16.0)		468	165 (7.1)	303 (13.1)		344	63 (3.4)	281 (15.3)		344	165 (9.0)	179 (9.7)	
LU	558	103 (4.4)	455 (19.6)		558	234 (10.1)	324 (14.0)		453	75 (4.1)	378 (20.6)		453	234 (12.7)	219 (11.9)	
LL	416	83 (3.6)	333 (14.4)		416	189 (8.2)	227 (9.8)		348	57 (3.1)	291 (15.8)		348	189 (10.3)	159 (8.7)	
Surgical Procedure				0.170				0.000				–				–
Lobectomy	2163	460 (19.9)	1703 (73.5)		2163	918 (39.6)	1245 (53.7)		1836	372 (20.3)	1464 (79.7)		1836	918 (50.0)	918 (50.0)	
Sublobar resection	154	40 (1.7)	114 (4.9)		154	0 (0.0)	154 (6.6)		–	–	–		–	–	–	
T stage				0.000				0.000				0.000				1.000
T1a	1301	182 (7.9)	1119 (48.3)		1301	582 (25.1)	719 (31.0)		1164	158 (8.6)	1006 (54.8)		1164	582 (31.7)	582 (31.7)	
T1b	716	179 (7.7)	537 (23.2)		716	240 (10.4)	476 (20.5)		480	133 (7.2)	347 (18.9)		480	240 (13.1)	240 (13.1)	
T1c	300	139 (6.0)	161 (6.9)		300	96 (4.1)	204 (8.8)		192	81 (4.4)	111 (6.0)		192	96 (5.2)	96 (5.2)	

(*continued on next page*)

Table 1 (*continued*)

Variables	Before PSM (n = 3061)								After PSM (n = 1836)							
	STAS				CT-guided Hookwire Localization				STAS				CT-guided Hookwire Localization			
	No. of patients	Present (%)	Absent (%)	*P* value	No. of patients	With (%)	Without (%)	*P* value	No. of patients	Present (%)	Absent (%)	*P* value	No. of patients	With (%)	Without (%)	*P* value
Growth Pattern of IAC				0.000				0.001				0.000				0.789
Lepidic predominant	747	78 (3.4)	669 (28.9)		747	339 (14.6)	408 (17.6)		657	56 (3.1)	601 (32.7)		657	339 (18.5)	318 (17.3)	
Acinar predominant	638	56 (2.4)	582 (25.1)		638	225 (9.7)	413 (17.8)		458	36 (2.0)	422 (23.0)		458	225 (12.3)	233 (12.7)	
Papillary predominant	353	31 (1.3)	322 (13.9)		353	145 (6.3)	208 (9.0)		286	25 (1.4)	261 (14.2)		286	145 (7.9)	141 (7.7)	
Micropapillary predominant	310	186 (8.0)	124 (5.4)		310	116 (5.0)	194 (8.4)		246	150 (8.2)	96 (5.2)		246	116 (6.3)	130 (7.1)	
Solid predominant	269	149 (6.4)	120 (5.2)		269	93 (4.0)	176 (7.6)		189	105 (5.7)	84 (4.6)		189	93 (5.1)	96 (5.2)	
Presence of STAS				–				0.013				–				0.163
Present	–	–	–		500	174 (7.5)	326 (14.1)		–	–	–		372	174 (9.5)	198 (10.8)	
Absent	–	–	–		1817	744 (32.1)	1073 (46.3)		–	–	–		1464	744 (40.5)	720 (39.2)	
Morphological Subtypes of STAS				–				0.003				–				0.653
Single Cells	100	100 (4.3)	–		100	21 (0.9)	79 (3.4)		50	50 (2.7)	–		50	21 (1.1)	29 (1.6)	
Micropapillary Clusters	230	230 (9.9)	–		230	83 (3.6)	147 (6.3)		180	180 (9.8)	–		180	83 (4.5)	97 (5.3)	
Solid Nests	170	170 (7.3)	–		170	70 (3.0)	100 (4.3)		142	142 (7.7)	–		142	70 (3.8)	72 (3.9)	
Consistency between STAS Morphology and Growth Pattern of Main Tumor				–				0.144				–				0.703
Inconsistent	295	295 (12.7)	–		295	95 (4.1)	200 (8.6)		207	207 (11.3)	–		207	95 (5.2)	112 (6.1)	
Consistent	205	205 (8.8)	–		205	79 (3.4)	126 (5.4)		165	165 (9.0)	–		165	79 (4.3)	86 (4.7)	
Hook-wire Localization				0.013				–				0.163				–
Without	1399	326 (14.1)	1073 (46.3)		–	–	–		918	198 (10.8)	720 (39.2)		–	–	–	
With	918	174 (7.5)	744 (32.1)		–	–	–		918	174 (9.5)	744 (40.5)		–	–	–	
CT-based Distance from Localization Site to Main Tumor				0.000				–				0.000				–
Non-adjacent	557	61 (2.6)	496 (21.4)		556	556 (24.0)	–		556	61 (3.3)	495 (27.0)		556	556 (30.3)	–	
Contiguous	240	75 (3.2)	165 (7.1)		240	240 (10.4)	–		240	75 (4.1)	165 (9.0)		240	240 (13.1)	–	
Penetrated	122	38 (1.6)	84 (3.6)		122	122 (5.3)	–		122	38 (2.1)	84 (4.6)		122	122 (6.6)	–	

Abbreviations: PSM, Propensity-Score Matching; STAS, Spread Through Air Spaces; CT, Computed Tomography; RU, Right Upper; RM, Right Middle; RL, Right Lower; LU, Left Upper; LL, Left Lower; IAC, Invasive Adenocarcinoma.

[18]. Notably, STAS was distinguished from alveolar macrophages and specimen sectioning artifacts using the methods described by Kadota et al. [1]. We also paid special attention to differentiating STAS from artifacts as reported in a previous study [7]. Briefly, immunohistochemical staining was employed to recognize and identify alveolar macrophages and real STAS with CD68 used as the marker for macrophages and AE1/3 for malignant epithelials [19–23]. Additionally, STAS was graded with a two-tiered system (STAS I: <2500 μm from the edge of tumor and STAS II: ≥2500 μm from the edge of tumor) using the criteria proposed by Han et al. [6].

2.6. Postoperative follow-up

Patients were followed up every 3 months for the first year after surgery and at 6-month intervals thereafter. For patients who were followed up at local health facilities, survival status and examination results were collected by telephone or email. Tumor locoregional recurrence or distant metastasis was diagnosed using chest CT, brain magnetic resonance imaging, and bone scintigraphy as well as ultrasound and/or abdominal CT. A PET–CT scan was suggested if possible. RFS was defined as the length of time from surgery to tumor recurrence or the last follow-up. OS was defined as the time from the surgical resection until death from any cause or the last follow up.

2.7. Statistical analysis

Data collection and all statistical analyses were performed with IBM SPSS software (Version 25.0, IBM Corp., NY, USA). Patient characteristics were reported as median and ranges or percentages. The chi-squared or Fisher's exact test was used to test differences. PSM was used to match the two patient groups stratified by implementation of CT-guided hookwire localization. The propensity score was calculated using logistic regression based on 6 clinicopathological characteristics (age, gender, smoking history, radiological feature, surgical procedure and T stage) that were thought to potentially affect the selection of localization and presence of STAS. Patients in the hookwire localization and control groups were matched in a 1:1 ratio according to their propensity score, and the caliper value was set to 0.02 to ensure optimal matching. Subsequent statistical analyses were performed using the matched groups. Associations between clinicopathological characteristics were analyzed using the Pearson $\chi 2$ test or Fisher's exact test for categorical variables and OS were evaluated using the Kaplan–Meier method, and nonparametric group comparisons were performed using the log-rank test. A P value less than 0.05 was considered statistically significant.

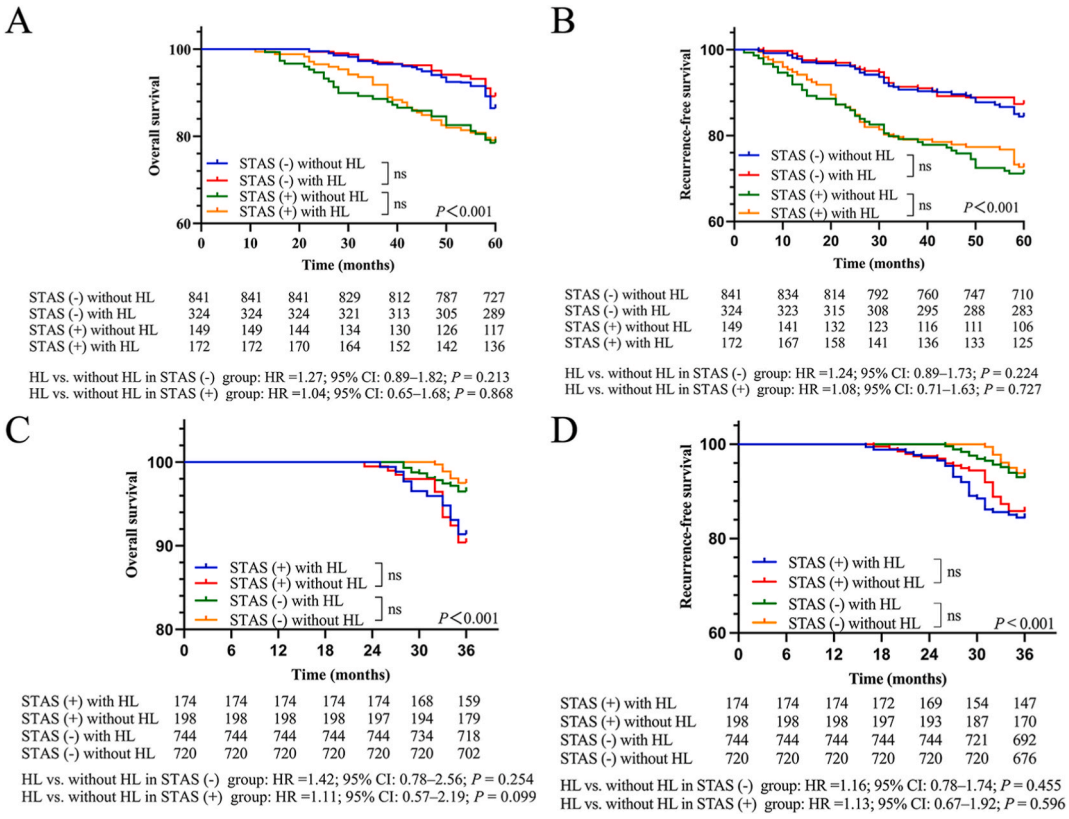

Fig. 1. OS and RFS of patients with p-stage IA lung adenocarcinoma receiving CT-guided hookwire localization after SR in the external cohort (A–B) and those receiving lobectomy in the primary cohort after PSM (*C*–D).

3. Results

3.1. Penetration via hookwire localizer ex vivo produced STALS

20 gross specimens receiving R0 resection were included in the ex vivo tests. Among them, presence of STALS were observed in the precancerous tissues in 17 specimens. AE1/3 broad-spectrum was used to identify epithelial components. Interestingly, AE1/3-positive cells were seen in none of the 17 STALS, whereas CD68-labeled cells were observed in all of them. In other words, all the STALS were macrophage-derived artifacts instead of real STAS (Supplemental Figs. 1C–D). In addition, the median distance between tumor and the furthest STALS was measured microscopically as 0.953 mm (range, 0.3–1.8 mm).

3.2. Clinicopathological characteristics of the primary cohort

A total of 1662 patients who underwent CT-guided hookwire localization were initially included in our study. Meanwhile, 1399 patients with IAC who did not receive CT-guided hookwire localization were also included for matching. PSM was employed to eliminate potential selection biases between the HL group and the control group. 918 patients with IAC in each group were finally matched. Baseline clinicopathological characteristics of the matched groups stratified by presence of STAS and CT-guided hookwire localization are summarized in Table 1. Presence of STAS was found in 174 (9.5 %) and 198 (10.8 %) patients in the HL and the control groups, respectively ($P = 0.163$). Survival analysis also indicated that hookwire localization was not associated with worse survival both in STAS-positive and -negative patients (Fig. 1C–D). Notably, the morphological subtypes of STAS (Fig. 2A–C) were not statistically significantly different between the HL and the control groups ($P = 0.653$) (Table 1). The HL group was also categorized into three subgroups according to the relative spatial position relations between localization site and main tumor, entitled as penetrated (6.6 %) (Supplemental Figs. 2A–B), contiguous (13.1 %) (Supplemental Figs. 3A–B) and non-adjacent (30.3 %) (Supplemental Figs. 4A–B).

3.3. Prognostic implications of hookwire localization on stage IA patients

The clinicopathological characteristics of the external patient cohort are shown in Supplemental Table 1. A total of 1486 patients

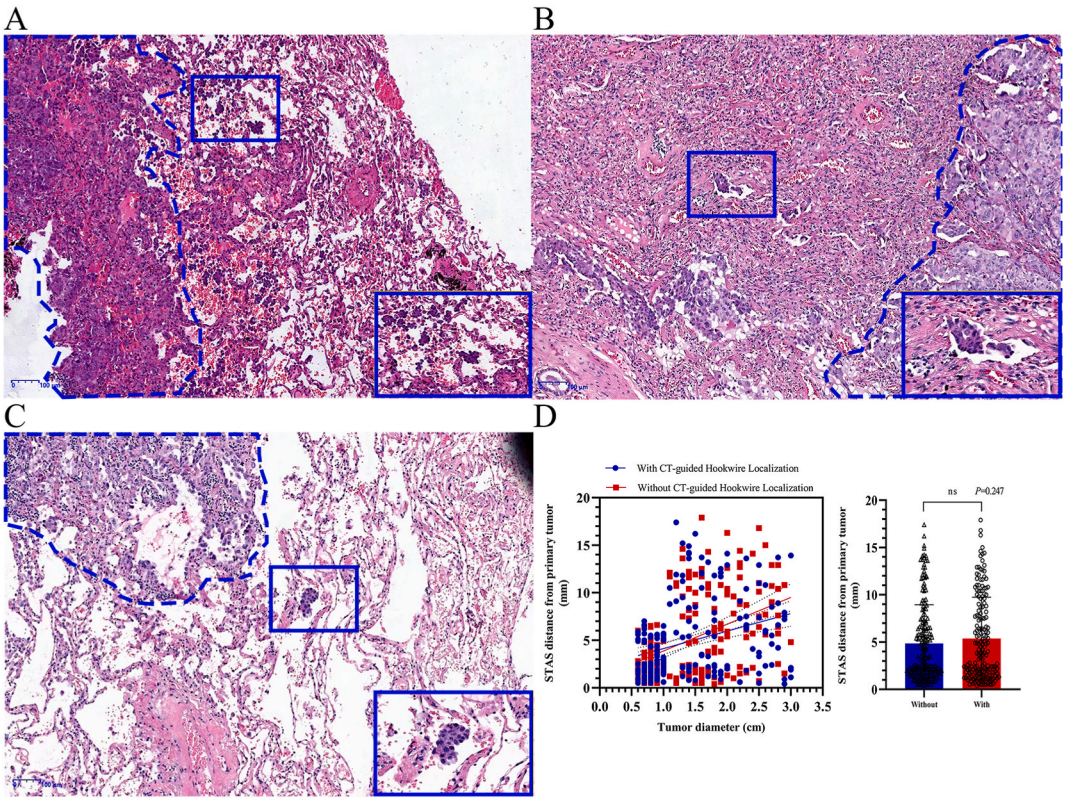

Fig. 2. Illustration of morphological subtypes of STAS, including single cell pattern(A), micropapillary pattern(B) and solid nest pattern(C). The relationship between the spreading distance from tumor edge and tumor diameter(D). Hematoxylin and eosin staining, original magnification: (A) × 10; (B) × 10; (C) × 10.

were included, among whom 496 (33.4 %) underwent CT-guided hookwire localization. Presence of STAS was identified in 321 (21.6 %) patients in the entire cohort. There was no significant difference in histologic patterns between the hookwire localization (HL) group and the control groups ($P = 0.235$). Interestingly, it was suggested that the incidence of STAS was higher in the HL group (11.6 %) compared with that in the control group (10.0 %) ($P < 0.001$). Survival analysis not only confirmed that presence of STAS was associated with worse RFS and OS after SR, but also revealed that implementation of HL affected the prognosis of neither STAS-negative patients nor -positive ones undergoing SR (Fig. 1A–B).

3.4. Association between preoperative hookwire localization and presence of STAS

To investigate the relationship between CT-guided hookwire localization and STAS, we further investigated all the 1662 patients who received CT-guided hookwire localization during the same period. After independent review of all sections by two pathologists and exclusion of the false positives, it was confirmed that STAS was merely available in IAC but not in MIA or AIS (Supplemental Table 2). Although no significant association was observed between hookwire localization and presence of STAS (Supplemental Table 3), it was revealed that presence of STAS might correlate with CT-based distance from localization site to main tumor (Supplemental Table 4). Therefore, logistic regression analysis was performed to determine potential factors associated with presence of STAS (Table 2). It was observed that radiologically solid nodule, larger tumor size and high-grade growth pattern were independent predictors of STAS, which clarified the insignificant association between CT-based distance from localization site to main tumor and presence of STAS with confounding factors adjusted.

3.5. CT-guided hookwire localization did not affect the consistency between morphological subtypes of STAS and growth patterns of main tumors

Firstly, we identified moderate correlation between the morphological subtypes of STAS and growth patterns of main tumors (Supplemental Table 5). To be noted, the consistency between STAS subtypes and growth patterns of main tumors was similar between the HL (79/174) and the control (86/198) groups (45.4 % vs. 43.4 %, $P = 0.703$) (Supplemental Table 6). Moreover, CT-based distance from localization site to main tumor (penetrated, contiguous, and non-adjacent) was proved not to be a determinant that affected the aforementioned consistency (spearman = 0.000, $P = 0.996$, Supplemental Table 7) (Supplemental Figs. 2C–D, Supplemental Figs. 3C–D, Supplemental Figs. 4C–D).

3.6. STAS distance and relative spatial position relations between localization site and main tumor

In terms of the spreading distance from the tumor edge, the farthest STAS could be found 17.9 mm away from the main tumor with a median of 3.5 ± 4.228 mm. In addition, our analysis indicated that the spreading distance from tumor edge was not associated with tumor diameter ($P = 0.247$, Fig. 2D), but correlated with CT-based distance from localization site to main tumor (spearman = 0.281, $P = 0.000$, Supplemental Table 8). Nonetheless, the logistic regression analysis identified that high-grade pattern rather than CT-based distance from localization site to main tumor was an independent predictor of the spreading distance of detached cells away from tumor edge (Table 3).

Table 2
Logistic regression analysis of risk factors for presence of STAS after PSM.

Variables	Univariable		Multivariable	
	OR (95 % CI)	*P* value	OR (95 % CI)	*P* value
Male sex (vs. female)	0.994 (0.791–1.248)	0.958	0.585 (0.334–1.025)	0.061
Age	1.099 (0.875–1.381)	0.415	0.672 (0.411–1.101)	0.114
Current or former smoker (vs. Non-smoker)	1.646 (1.289–2.102)	0.000	1.228 (0.676–2.232)	0.500
Radiological feature				
Solid (vs. Subsolid)	2.219 (1.744–2.824)	0.000	4.726 (2.836–7.874)	0.000
T stage				
T1b stage (vs. T1a stage)	2.440 (1.880–3.168)	0.000	3.157 (1.594–6.253)	0.001
T1c stage (vs. T1a stage)	4.646 (3.334–6.475)	0.000	4.053 (1.684–9.753)	0.002
Growth Pattern of IAC				
Acinar predominant (vs. Lepidic predominant)	0.916 (0.592–1.417)	0.692	0.551 (0.231–1.313)	0.179
Papillary predominant (vs. Lepidic predominant)	1.028 (0.628–1.684)	0.913	2.119 (0.889–5.052)	0.090
Micropapillary predominant (vs. Lepidic predominant)	16.769 (11.525–24.398)	0.000	47.890 (23.874–96.065)	0.000
Solid predominant (vs. Lepidic predominant)	13.415 (9.023–19.946)	0.000	20.110 (10.081–40.117)	0.000
CT-based Distance from Localization Site to Main Tumor				
Contiguous (vs. Non-adjacent)	3.689 (2.520–5.400)	0.000	1.831 (0.937–3.575)	0.077
Penetrated (vs. Non-adjacent)	3.671 (2.303–5.853)	0.000	2.039 (0.918–4.529)	0.080

Abbreviations: STAS, Spread Through Air Spaces; PSM, Propensity-Score Matching; OR, Odds Ratio; 95%CI, 95 % Confidence Interval; IAC, Invasive Adenocarcinoma; CT, Computed Tomography.

Table 3
Logistic regression analysis of risk factors for grade of STAS after PSM.

Variables	Univariable		Multivariable	
	OR (95 % CI)	*P* value	OR (95 % CI)	*P* value
Male sex (vs. female)	1.258 (0.835–1.897)	0.272	0.960 (0.436–2.118)	0.920
Age	0.916 (0.608–1.380)	0.675	1.131 (0.570–2.242)	0.725
Current or former smoker (vs. Non-smoker)	1.026 (0.667–1.577)	0.908	1.620 (0.671–3.910)	0.284
Radiological feature				
Solid (vs. Subsolid)	1.282 (0.841–1.954)	0.248	1.395 (0.684–2.845)	0.360
T stage				
T1b stage (vs. T1a stage)	2.928 (1.814–4.729)	0.000	2.051 (0.695–6.049)	0.193
T1c stage (vs. T1a stage)	4.424 (2.451–7.986)	0.000	2.702 (0.890–8.205)	0.079
Growth Pattern of IAC				
Acinar predominant (vs. Lepidic predominant)	0.714 (0.269–1.896)	0.499	1.267 (0.194–8.254)	0.805
Papillary predominant (vs. Lepidic predominant)	1.667 (0.620–4.477)	0.311	1.919 (0.310–11.901)	0.484
Micropapillary predominant (vs. Lepidic predominant)	6.023 (3.057–11.864)	0.000	4.658 (1.402–15.478)	0.012
Solid predominant (vs. Lepidic predominant)	4.792 (2.365–9.708)	0.000	5.416 (1.515–19.360)	0.009
CT-based Distance from Localization Site to Main Tumor				
Contiguous (vs. Non-adjacent)	2.239 (1.122–4.468)	0.022	1.263 (0.428–3.733)	0.672
Penetrated (vs. Non-adjacent)	3.091 (1.303–7.335)	0.010	2.091 (0.671–6.523)	0.204

Abbreviations: STAS, Spread Through Air Spaces; PSM, Propensity-Score Matching; OR, Odds Ratio; 95%CI, 95 % Confidence Interval; IAC, Invasive Adenocarcinoma; CT, Computed Tomography.

4. Discussion

With the popularization of low-dose CT, lung adenocarcinomas presenting as peripheral pulmonary nodules are increasingly detected, especially ground-glass nodules (GGNs). The advent of VATS has provided a minimally invasive approach for diagnosis and treatment of pulmonary nodules [17]. Meanwhile, the possibly intraoperative invisibility and imperceptibility of GGNs have highlighted the importance of preoperative localization of the lesions. However, it remains undetermined regarding the relationships between preoperative hookwire localization and presence of STAS in stage IA IAC.

A previous study revealed micropapillary cluster and solid nest STAS to be an independent predictor of worse RFS and OS, but not for single cell STAS, which suggested single-cell STAS as a common morphologic type of artifacts produced by a prosecting knife [24]. Nonetheless, another study highlighted that there was no difference between STAS occurrence in freshly cut and fixed corresponding samples [25], which indicated STAS as a phenomenon preexisting in surgical tissue processing. In addition to the real phenomenon that consecutive knife cuts and subsequent carryover increased STAS-like free-floating tumor clusters with each sequential cut, if the knife was not cleaned between the cuts [25], the detachment of tumor cell clusters might arise from multiple mechanical factors. A recent study has shown preoperative biopsy in stage I NSCLC was neither associated with an elevated risk of STAS nor influenced the prognosis related to STAS [26]. In our present study, CT-guided hookwire localization did not bring additional risk in presence of STAS. Although CT-based distance from localization site to main tumor was suspected to be associated with presence of STAS in the univariate logistic analysis, it could be explained as most pulmonary nodules in the penetrated subgroup had a larger size which acted as an independent predictor of STAS presence. Similar condition was also seen regarding the risk factors for grade of STAS. Furthermore, the aforementioned distance had hardly any correlation with the consistency between STAS subtypes and growth patterns of main tumors. Despite JCOG0802 [7] as well as CALGB140503 [8] in which patients with clinical T1N0M0 NSCLC undergoing SR had similar outcomes to those undergoing lobectomy, it is worth noting that information on preoperative localization and STAS was unavailable in both trials. From our data, STAS remained as an adverse prognosticator after SR even in stage IA disease. Interestingly, our study also suggested that although STALS might be mistaken as STAS in sections, immunochemical staining using CD68 and AE1/3 antibodies could be helpful in distinguishing them. Additionally, the distance of STALS dissemination tended to be relatively short ($P = 0.000$). More importantly, implementation of hookwire localization did not lead to worse survival in stage IA patients receiving SR. In a word, less concern might be shown regarding localization-caused tumor dissemination in stage IA patients for whom intentional SR is a suitable procedure.

There were several limitations to this study. First, lack of external validation from other centers possibly impaired the robustness of our results. Second, the retrospective nature of our study might lead to selection and performance bias even though PSM was employed, and the results from randomized controlled trials might be more convincing. Third, the number of STAS-positive patients was limited in the HL group, which might pose an obstacle for our further subgroup analyses.

5. Conclusion

CT-guided hookwire localization might induce mechanical artifacts presenting as STALS which could be distinguished by immunohistochemistry. Hookwire localization was not a prognosticator in p-stage IA disease irrespective of STAS presence. Surgeons can be less apprehensive about performing hookwire localization in relation to STAS on stage IA disease suitable for SR.

Ethics statement

The ethics committee of the Second Affiliated Hospital of Soochow University approved this study (IRB: JD-HG-2022-25).

Data availability statement

The data that support the findings of this study are available from the corresponding author upon reasonable request.

Funding statement

The study was supported by Jiangsu Key Research and Development Plan (Social Development) Project (BE2020653), Key Scientific Program of Jiangsu Provincial Health Commission (ZD2021033), Gusu Health Leading Talent Program of Suzhou (GSWS2021020), Discipline Construction Project of the Second Affiliated Hospital of Soochow University (XKTJ-XK202004), Discipline Construction Project of the Second Affiliated Hospital of Soochow University - Key Talent Project for Medical Application of Nuclear Technology (XKTJHRC20210014) and Youth Funding of Zhongshan Hospital (Residency 2022-007).

CRediT authorship contribution statement

Xiaofan Wang: Writing – original draft, Formal analysis, Data curation. **Xiaoxiao Dai:** Resources, Formal analysis. **Qifeng Ding:** Validation. **Yi Xu:** Investigation. **Lei Chen:** Investigation. **Shanzhou Duan:** Validation. **Yongsheng Zhang:** Writing – review & editing. **Yongbing Chen:** Writing – review & editing, Resources. **Donglai Chen:** Writing – review & editing, Validation, Supervision.

Declaration of competing interest

The authors declare that they have no known competing financial interests or personal relationships that could have appeared to influence the work reported in this paper.

Appendix A. Supplementary data

Supplementary data to this article can be found online at https://doi.org/10.1016/j.heliyon.2023.e23705.

References

[1] K. Kadota, J.I. Nitadori, C.S. Sima, et al., Tumor spread through air spaces is an important pattern of invasion and impacts the frequency and location of recurrences after limited resection for small stage I lung adenocarcinomas, J. Thorac. Oncol. 10 (5) (2015) 806–814, https://doi.org/10.1097/jto.0000000000000486.
[2] H. Blaauwgeers, D. Flieder, A. Warth, et al., A prospective study of loose tissue fragments in non-small cell lung cancer resection specimens: an alternative view to "spread through air spaces", Am. J. Surg. Pathol. 41 (9) (2017) 1226–1230, https://doi.org/10.1097/pas.0000000000000889.
[3] H. Liu, Q. Yin, G. Yang, et al., Prognostic impact of tumor spread through air spaces in non-small cell lung cancers: a meta-analysis including 3564 patients, Pathol. Oncol. Res. 25 (4) (2019) 1303–1310, https://doi.org/10.1007/s12253-019-00616-1.
[4] A.R. Shih, M. Mino-Kenudson, Updates on spread through air spaces (STAS) in lung cancer, Histopathology 77 (2) (2020) 173–180, https://doi.org/10.1111/his.14062.
[5] D. Chen, Y. Mao, J. Wen, et al., Tumor spread through air spaces in non-small cell lung cancer: a systematic review and meta-analysis, Ann. Thorac. Surg. 108 (3) (2019) 945–954, https://doi.org/10.1016/j.athoracsur.2019.02.045.
[6] Y.B. Han, H. Kim, M. Mino-Kenudson, et al., Tumor spread through air spaces (STAS): prognostic significance of grading in non-small cell lung cancer, Mod. Pathol. 34 (3) (2021) 549–561, https://doi.org/10.1038/s41379-020-00709-2.
[7] H. Saji, M. Okada, M. Tsuboi, et al., Segmentectomy versus lobectomy in small-sized peripheral non-small-cell lung cancer (JCOG0802/WJOG4607L): a multicentre, open-label, phase 3, randomised, controlled, non-inferiority trial, Lancet 399 (10335) (2022 Apr 23) 1607–1617, https://doi.org/10.1016/s0140-6736(21)02333-3.
[8] N.K. Altorki, X. Wang, D. Wigle, et al., Perioperative mortality and morbidity after sublobar versus lobar resection for early-stage non-small-cell lung cancer: post-hoc analysis of an international, randomised, phase 3 trial (CALGB/Alliance 140503), Lancet Respir. Med. 6 (12) (2018 Dec) 915–924, https://doi.org/10.1016/s2213-2600(18)30411-9.
[9] T. Eguchi, K. Kameda, S. Lu, et al., Lobectomy is associated with better outcomes than sublobar resection in spread through air spaces (STAS)-Positive T1 lung adenocarcinoma: a propensity score-matched analysis, J. Thorac. Oncol. 14 (1) (2019 Jan) 87–98, https://doi.org/10.1016/j.jtho.2018.09.005.
[10] C. Dai, H. Xie, H. Su, et al., Tumor spread through air spaces affects the recurrence and overall survival in patients with lung adenocarcinoma >2 to 3 cm, J. Thorac. Oncol. 12 (7) (2017 Jul) 1052–1060, https://doi.org/10.1016/j.jtho.2017.03.020.
[11] Y. Ren, H. Xie, C. Dai, et al., Prognostic impact of tumor spread through air spaces in sublobar resection for 1A lung adenocarcinoma patients, Ann. Surg Oncol. 26 (6) (2019 Jun) 1901–1908, https://doi.org/10.1245/s10434-019-07296-w.
[12] M.B. Amin, S.B. Edge, F.L. Greene, et al., AJCC Cancer Staging Manual, eighth ed., Springer, Chicago, USA, 2017 https://doi.org/10.3322/caac.21388.
[13] L. Zhang, L. Wang, X. Kadeer, et al., Accuracy of a 3-dimensionally printed navigational template for localizing small pulmonary nodules: a noninferiority randomized clinical trial, JAMA Surg 154 (4) (2019) 295–303, https://doi.org/10.1001/jamasurg.2018.4872.
[14] J. Ichinose, T. Kohno, S. Fujimori, et al., Efficacy and complications of computed tomography-guided hook wire localization, Ann. Thorac. Surg. 96 (4) (2013) 1203–1208, https://doi.org/10.1016/j.athoracsur.2013.05.026.
[15] T.J. Klinkenberg, L. Dinjens, R.F.E. Wolf, et al., CT-guided percutaneous hookwire localization increases the efficacy and safety of VATS for pulmonary nodules, J. Surg. Oncol. 115 (7) (2017) 898–904, https://doi.org/10.1002/jso.24589.

[16] Q. Ding, D. Chen, X. Wang, et al., Characterization of lung adenocarcinoma with a cribriform component reveals its association with spread through air spaces and poor outcomes, Lung Cancer 134 (2019) 238–244, https://doi.org/10.1016/j.lungcan.2019.06.027.
[17] M. Congregado, R.J. Merchan, G. Gallardo, et al., Video-assisted thoracic surgery (VATS) lobectomy: 13 years' experience, Surg. Endosc. 22 (8) (2008) 1852–1857, https://doi.org/10.1007/s00464-007-9720-z.
[18] W.D. Travis, E. Brambilla, A.G. Nicholson, et al., The 2015 world health organization classification of lung tumors: impact of genetic, clinical and radiologic advances since the 2004 classification, J. Thorac. Oncol. 10 (9) (2015) 1243–1260, https://doi.org/10.1097/jto.0000000000000630.
[19] K. Inamura, Clinicopathological characteristics and mutations driving development of early lung adenocarcinoma: tumor initiation and progression, Int. J. Mol. Sci. 19 (4) (2018 Apr 23) 1259, https://doi.org/10.3390/ijms19041259.
[20] D. Jain, A. Nambirajan, A. Borczuk, et al., Immunocytochemistry for predictive biomarker testing in lung cancer cytology, Cancer Cytopathol 127 (5) (2019 May) 325–339, https://doi.org/10.1002/cncy.22137.
[21] Y. Yatabe, S. Dacic, A.C. Borczuk, et al., Best practices recommendations for diagnostic immunohistochemistry in lung cancer, J. Thorac. Oncol. 14 (3) (2019 Mar) 377–407, https://doi.org/10.1016/j.jtho.2018.12.005.
[22] Y. Qiu, H. Yang, H. Chen, et al., Detection of CEA mRNA, p53 and AE1/AE3 in haematoxylin-eosin-negative lymph nodes of early-stage non-small cell lung cancer may improve veracity of N staging and indicate prognosis, Jpn. J. Clin. Oncol. 40 (2) (2010 Feb) 146–152, https://doi.org/10.1093/jjco/hyp144.
[23] A. Badzio, P. Czapiewski, A. Gorczyński, et al., Prognostic value of broad-spectrum keratin clones AE1/AE3 and CAM5.2 in small cell lung cancer patients undergoing pulmonary resection, Acta Biochim. Pol. 66 (1) (2019 Feb 22) 111–114, https://doi.org/10.18388/abp.2018_2773.
[24] H. Xie, H. Su, E. Zhu, et al., Morphological subtypes of tumor spread through air spaces in non-small cell lung cancer: prognostic heterogeneity and its underlying mechanism, Front. Oncol. 11 (2021), 608353, https://doi.org/10.3389/fonc.2021.608353.
[25] J. Metovic, E.C. Falco, E. Vissio, et al., Gross specimen handling procedures do not impact the occurrence of spread through air spaces (STAS) in lung cancer, Am. J. Surg. Pathol. 45 (2) (2021) 215–222, https://doi.org/10.1097/pas.0000000000001642.
[26] G.Y. Lee, J.H. Chung, S. Cho, et al., Impact of preoperative diagnostic biopsy procedure on spread through airspaces and related outcomes in resected stage I non-small cell lung cancer, Chest S0012–3692 (22) (2022), https://doi.org/10.1016/j.chest.2022.05.002, 00897-2.